Published in final edited form as:
J Am Chem Soc. 2010 May 5; 132(17): 6001–6005. doi:10.1021/ja9063074.

Nature of Intermediates in Organo-SOMO Catalysis of α-Arylation of Aldehydes

Joann M. Um[‡], **Osvaldo Gutierrez**[‡], **Franziska Schoenebeck**[‡], **K. N. Houk**[‡], and **David W. C. MacMillan**[†]

K. N. Houk: houk@chem.ucla.edu; David W. C. MacMillan: dmacmill@princeton.edu

[‡] Department of Chemistry and Biochemistry, University of California, Los Angeles, CA 90095-1569

[†] Merck Center for Catalysis at Princeton University, Princeton, New Jersey 08544

Abstract

The intramolecular α-arylation of aldehydes via organo-SOMO catalysis was investigated using density functional theory (B3LYP and M06-2X functionals). The geometries, spin densities, Mulliken charges, and molecular orbitals of the reacting enamine radical cations were analyzed, and the nature of the resulting cyclized radical cation intermediates were characterized. In agreement with experimental observations, the calculated 1,3-disubstituted aromatic system shows *ortho* selectivity, while the 1,3,4-trisubstituted systems show *para, meta* (instead of *ortho, meta*) selectivity. The selectivity change for the trisubstituted rings is attributed to a distortion of the *ortho* substituents in the *ortho, meta* cyclization transition structures, causing a destabilization of these isomers and therefore selectivity for the *para, meta* product.

Introduction

Organo-SOMO catalysis has recently become an important activation mode for the asymmetric α-allylation,[1a] α-enolation,[1b] α-vinylation,[1c] α-carbo-oxidation,[1d] α-nitroalkylation[1e] and intramolecular α-arylation1f–g,[2] of aldehydes. One of our groups has shown that the reactions proceed via a 3π-electron radical cation species, generated by the one-electron oxidation of a chiral enamine. In a report of the intramolecular α-arylation reactions from the Nicolaou group1f,g and our laboratory,[2] the cyclization of enamine radical cation **4** was shown to selectively attack *ortho* to the methoxy group (Scheme 1).[3,4] It was proposed that an intermediate best represented as **5**, rather than **6**, described earlier,1f–g was involved. The Nicolaou group showed that 1,3,4-trisubstituted aldehydes **8–10**, however, react to give *para* aryl products **11–13** (Scheme 2). We have explored the mechanisms of these reactions, particularly the nature of the intermediates and origins of selectivity using quantum mechanical calculations.[5]

Results and Discussion

UB3LYP calculations were performed on the simple model radical cation **14***. Bond distances, spin densities, Mulliken charges, and singly occoupied molecular orbital (SOMO) coefficients of model radical cation **14*** are shown in Figure 1. The C1–C2 bond distance (1.39 Å) is longer than that of an enamine (1.34 Å), and the N-C1 distance (1.33 Å) is closer to that of an iminium

Correspondence to: K. N. Houk, houk@chem.ucla.edu; David W. C. MacMillan, dmacmill@princeton.edu.

Supporting information available: Cartesian coordinates and energies of all reported structures and model systems; full authorship of reference [5]. This material is available free of charge via the Internet at http://pubs.acs.org.

(1.29 Å) than of an enamine (1.40 Å). The majority of the spin is on the carbon β to the nitrogen (C2) and the charge is mainly on the iminium carbons α to the nitrogen, as in ammonium cations.[6] A molecular orbital analysis shows that the largest coefficient of the singly occupied π orbital (SOMO) lies on C2. The species is of course a resonance hybrid, **14**, but is best characterized as an alkyl radical conjugated to an iminium cation. The spin density is consistent with major contributions from **14a** and **14b**.

The enamine radical cation of propanal with catalyst **2** is similar (**15-*E****, Figure 2). The reported enantioselectivity range with this catalyst was 84–98%.1f,g,[2] The lowest-energy conformer is expected to direct attack from the less hindered *si* ("bottom") face of **15-*E****, which is in agreement with the experimentally observed stereoisomer.[3] The lowest-energy *Z* isomer **15-*Z****, which would give the opposite enantiomer of the product, is 3.0 kcal/mol higher in energy than **15-*E****.

Having established the charge and spin density distribution of the enamine radical cations, we investigated the transition structures for *para* and *ortho* attack of achiral radical cation **16*** on the anisole ring (Figure 3). In agreement with experimental results, *ortho* attack (**TS1***) is predicted to be favored over *para* attack (**TS2***) by 0.5 kcal/mol. The activation free energy for attack on the unsubstituted benzene is approximately 3 kcal/mol higher (18.3 kcal/mol), in agreement with the failed cyclization of this arene under the same reaction conditions.[7]

The endergonicities (**17*** and **18***) suggest that the cyclization step is easily reversible. Given that **17*** should accumulate in higher concentrations than **18***, the potential subsequent steps were explored. Deprotonation of the more abundant and faster formed **17*** leads to the favored ortho product. Oxidation of **17***, as suggested in ref. [2], was calculated to be at least as feasible as oxidation of the enamine that gives **16***.[8] Radical trapping of **17***, followed by deprotonation/aromatization and iminium hydrolysis, or trapping of the iminium by water,[9] followed by oxidation and subsequent deprotonation/aromatization and hydrolysis, are potential fates of the cyclized radical cations. Both of these trapping mechanisms are expected to occur readily with little rate dependence on *ortho/para* selectivity, so the greater stabilization of the cyclohexadienyl radical by the methoxy at the 1- rather than 3-position provides the basic origin of selectivity. Exactly the opposite would happen were the intermediate to have primarily cyclohexadienyl cation character. CBS-QB3 calculations of model 1- and 3-methoxy cyclohexadienyl cations (**19*** and **20***, respectively, Figure 4) show that the 3-methoxy cation (**20***) is 3.1 kcal/mol more stable than the 1-methoxy cation (**19***). This can be explained by the stabilization of the positive charge of **21*** at C3 by the methoxy group and a larger LUMO coefficient at this position. On the contrary, the 1-methoxy cyclohexadienyl radical (**22***) is 3.6 kcal/mol more stable than the 3-methoxy radical (**23***). Both the spin density and SOMO coefficient of **24*** are larger at C3 than at C1. Thus the explanation for the relative stabilities of cyclohexadienyl radicals requires more than a simple spin density or molecular orbital analysis.[10]

We next investigated the cyclization of aldehydes **8–10** via the model dimethyl enamine radical cations (Figures 5–7). Our calculations show that *para, meta* cyclization is favored over *ortho, meta* cyclization by 2.5–3.4 kcal/mol, in agreement with experiment. The intermediates, **26*****–27*****, 29*****–30***, and **32*****–33***, have the same predominantly cyclohexadienyl radical character as described for **17*** and **18***. The *para, meta* cyclization barriers **TS4*****, TS6*** and **TS8*** are similar to that of TS1* (approximately 15–16 kcal/mol), while the *ortho, meta* cyclization barriers **TS3*****, TS5*** and **TS7*** are larger than TS1* (approximately 18 kcal/mol). These results suggest that the *meta* substituent (R^4) causes the *ortho, meta* transition states to be destabilized. Given that the activation energies of **TS3*****, TS5*** and **TS7*** are similar to that of the unsubstituted system, it is possible that the *ortho, meta* cyclizations do not occur under the reaction conditions (−30 °C). M06-2X has been found to be reliable for weak dispersion

interactions and has had success with organic reactions involving radicals,[11] so we applied this method by applying single point calculations to the B3LYP optimized geometries. The results are summarized with the B3LYP energies in Table 1.

Compared to the B3LYP activation free energies, the M06-2X barriers are approximately 2–3 kcal/mol lower. The M06-2X reaction free energies are less endergonic than the B3LYP values by 4–7 kcal/mol. The calculated M06-2X selectivities are in good agreement with experimental observations and B3LYP predictions. For cyclization of monomethoxy radical cation **25***, the difference between **TS1*** and **TS2*** is 1.5 kcal/mol at the M06-2X level, compared to 0.5 kcal/mol using B3LYP. The *ortho* cyclized radical cation **17*** is 4.4 kcal/mol more stable than the *para* isomer **18*** using M06-2X. Of the 1,3,4-trisubstituted systems, **25*** and **31*** show a 2.3 kcal/mol selectivity for *para, meta* cyclization at the M06-2X level (**TS4*** versus **TS3*** and **TS8*** versus **TS7***), while **28*** shows a smaller selectivity of 1.3 kcal/mol (**TS6*** versus **TS5***). M06-2X calculations show little difference in the relative stabilities of *para, meta* cyclized radical cations **27*** and **30*** with respect to the *ortho, meta* isomers (**26*** and **29***, respectively). The *para, meta* radical cation **33*** is more stable than the *ortho, meta* isomer **32*** by 1.0 kcal/mol. Given the lack of stability difference between the *ortho, meta* and *para, meta* cyclized radical cations, and given the consistently high *ortho, meta* arylation activation barriers which are within 1.4 kcal/mol of the barrier for the unsubstituted aldehyde (which is completely unreactive), we conclude that the selectivity of 1,3,4-trisubstituted aldehydes **8–10** is controlled by the activation free energies.

The destabilization of *ortho, meta* transition states **TS3*, TS5***, and **TS7*** compared to *para, meta* isomers **TS4*, TS6*,** and **TS8*** can be explained by the conformation of the *meta* substituent R^3. It has been established that the methoxy groups of anisole prefer a planar conformation.[12] The same conformational preference holds true for *ortho* (**22***) and *para* (**23***) methoxy cyclohexadienyl radicals. In *ortho, meta* transition states **TS3*** and **TS5***, the *ortho* methoxy group cannot be planar due to steric hindrance from the *meta* R^4 group, raising the energies compared to the *para, meta* transition states. The *meta* oxygen of *ortho, meta* transition state **TS7*** is also nonplanar because the parent 1,3-benzodioxole prefers a non-planar conformation in which the methylene moiety is puckered with respect to the 5-membered ring.[13] This is due to the anomeric effect—stabilizing $n \rightarrow \sigma^*$ interactions between the oxygen lone pairs and C–O σ* orbitals of the puckered conformation. Electrostatic repulsion may exist between the oxygen lone pairs and the iminium moiety of the catalyst. This repulsion is relieved in cyclized radical cations **26*, 29*** and **32*** as the iminium group bends away from the cyclohexadienyl radical. (Compare dihedral angles a-b-c-d, Table 2).

In conclusion, the selectivity of the α-arylation reactions is attributed to the activation energies and relative stabilities of the isomeric transition states. In the case of the monomethoxy aryl system **1***, both *ortho* and *para* arylation barriers are possible under the reaction conditions. These reactions are endergonic, and the transition state energies are related to the relative stabilities of the resulting cyclized radical cation intermediates. For the more highly substituted **8*–10***, R^3 is distorted from planarity, which raises the energy of the *ortho, meta* transition states with respect to the *para, meta* isomers. The *ortho, meta* activation energies are similar to those of unreactive aldehydes. Thus, *ortho, meta* cyclization does not occur under the reaction conditions, resulting in the experimentally observed *para, meta* selectivity. A detailed study of the origins of the relative stabilities of cyclohexadienyl radicals is underway and will be reported in due course.

Supplementary Material

Refer to Web version on PubMed Central for supplementary material.

Acknowledgments

We are grateful to the National Institute of General Medical Sciences, National Institutes of Health (GM 36700, K.N.H. and R01 GM 078201-01-01, D.W.C.M.); Ronald S. Gabriel, M.D./Scrubs Unlimited SRF (O.G.); Novartis/ACS (J.M.U.); and Alexander von Humboldt foundation for a Feodor Lynen Fellowship (F.S.) for support of this work. Computations were performed on the NSF TeraGrid resources provided by NCSA (CHE0400414) and the UCLA Academic Technology Services (ATS) Hoffman2 and IDRE clusters.

References

1. (a) Beeson TD, Mastracchio A, Hong JB, Ashton K, MacMillan DWC. Science 2007;316:582. [PubMed: 17395791] (b) Jang HY, Hong JB, MacMillan DWC. J Am Chem Soc 2007;129:7004. [PubMed: 17497866] (c) Kim H, MacMillan DWC. J Am Chem Soc 2008;130:398. [PubMed: 18095690] (d) Graham TH, Jones CM, Jui NT, MacMillan DWC. J Am Chem Soc 2008;130:16494. [PubMed: 19049447] (e) Wilson JE, Casarez AD, MacMillan DWC. J Am Chem Soc 2009;131:11332. [PubMed: 19627154] (f) Nicolaou KC, Reingruber R, Sarlah D, Bräse S. J Am Chem Soc 2009;131:2086. [PubMed: 19173649] Correction: (g) J Am Chem Soc 2009;131:6640.
2. Conrad JC, Kong J, Laforteza BN, MacMillan DWC. J Am Chem Soc 2009;131:11640. [PubMed: 19639997]
3. The authors of ref. [1f] used (2*R*,5*R*)-2 as the catalyst. Because our calculations and experiments were performed with the opposite enantiomer, this paper reports the study of catalyst (2*S*,5*S*)-2.
4. For ortho-selective radical additions to aromatics, see: (a) Tiecco, M.; Testaferri, L. Reactive Intermediates. Abramovitch, RA., editor. Vol. 3. New York: Plenum Press; 1983. p. 61 (b) Guadarrama-Morales O, Mendéz F, Miranda LD. Tetrahedron Lett 2007;48:4515. (c) Muchowski JM, Cho IS, Jaime-Figueroa S, Artis RD. J Org Chem 1994;59:2456.For a study on the stability of cyclohexadienyl radicals, see: (d) Birch AJ, Hinde AL, Radom L. J Am Chem Soc 1980;102:4074.
5. With the exceptions of 14*, 15-*E**, 15-*Z** and 19*–24*, which were optimized in the gas phase, all geometries were optimized in water (CPCM model) using density functional theory, UB3LYP/6-31G (d), as implemented in the Gaussian03 suite of programs (Frisch, M. J.; et al. Gaussian 03, revision D. 01; Gaussian, Inc.: Pittsburgh, PA, 2004). Model cations and radicals 19*–24* were optimized using both CBS-QB3 (Gaussian 03) and UB3LYP/6-31G(d). All stationary points were verified by vibrational frequency analysis. Single point calculations were also performed using M06-2X/6-31+G (d) as implemented in Gaussian09. All computed structures are designated with an asterisk (*). The resulting energies are reported in all figures and schemes in kcal/mol.
6. (a) Olah GA, Prakash GKS, Rasul G. Chem Eur J 2009;15:8443. (b) No KT, Grant JA, Jhon MS, Scheraga HA. J Phys Chem 1990;94:4740. (c) Würthwein E-U, Sen KD, Pople JA, Schleyer Pv-R. Inorg Chem 1983;22:496.
7. Unpublished results.
8. See the Supporting Information.
9. For an example of water-assisted reactivity of radical cations, see: Heinemeann C, Demuth M. J Am Chem Soc 1999;121:4894.
10. This study is underway and will be reported in due course.
11. For examples, see: (a) Zhao Y, Truhlar DG. J Phys Chem A 2008;112:1095. [PubMed: 18211046] (b) Hohenstein EG, Chill ST, Sherrill CD. J Chem Theory Comput 2008;4:1996. (c) Valdes H, Pluháckova K, Pitonák M, Rezác J, Hobza P. Phys Chem Chem Phys 2008;10:2747. [PubMed: 18464990]
12. The preferred planar methoxy conformation holds true for anisole. For example, see: Emsley JW, Foord EK, Lindon JC. J Chem Soc, Perkin Trans 1998;2:1211.
13. (a) Sakurai S, Meinander N, Morris K, Laane J. J Am Chem Soc 1999;121:5056. (b) Moon S, Kwon Y, Lee J, Choo J. J Phys Chem A 2001;105:3221.

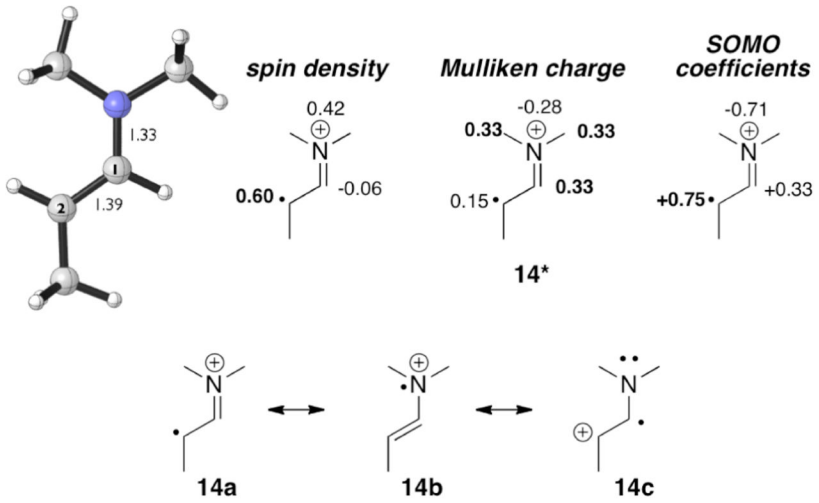

Figure 1.
Model enamine radical cation **14*** (UB3LYP/6-31G(d)).

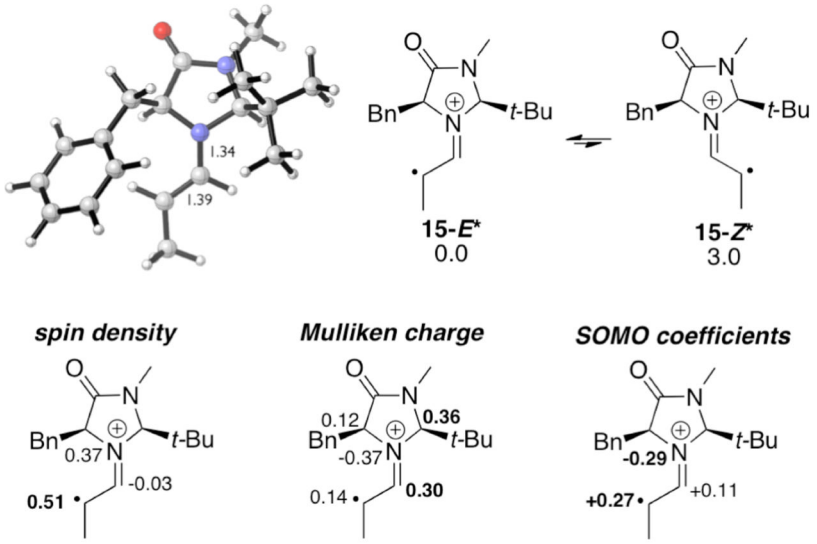

Figure 2.
Model enamine radical cation **15*** (UB3LYP/6-31G(d)).

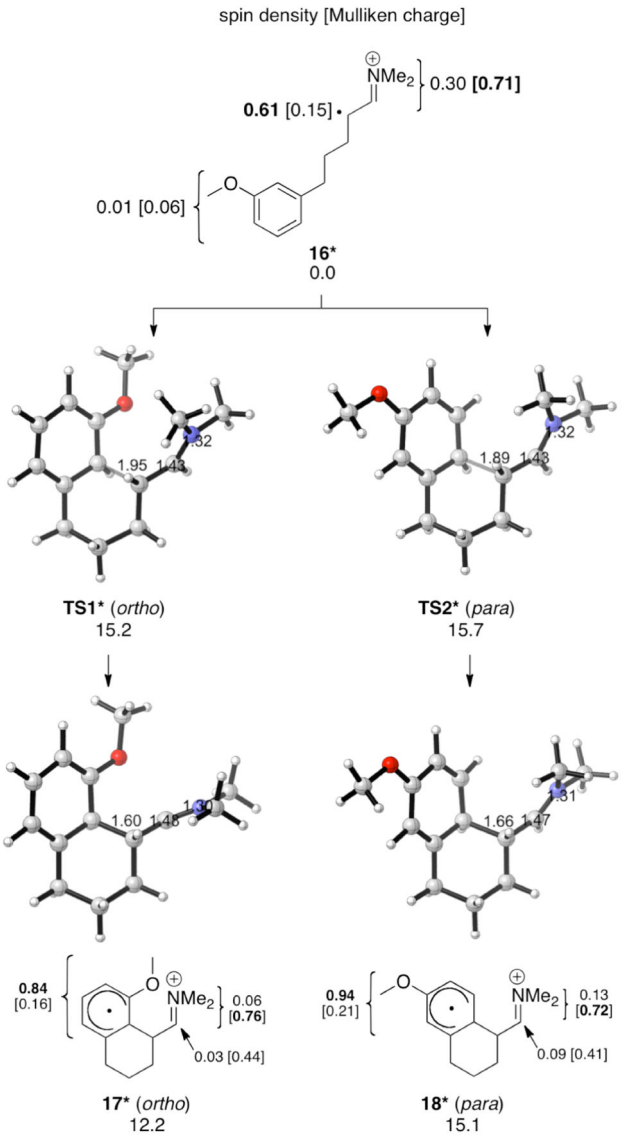

Figure 3.

Intramolecular α-arylation of **16*** (UB3LYP/6-31G(d) Δ*G* values for aqueous solution at 268 K; optimizations in CPCM water).

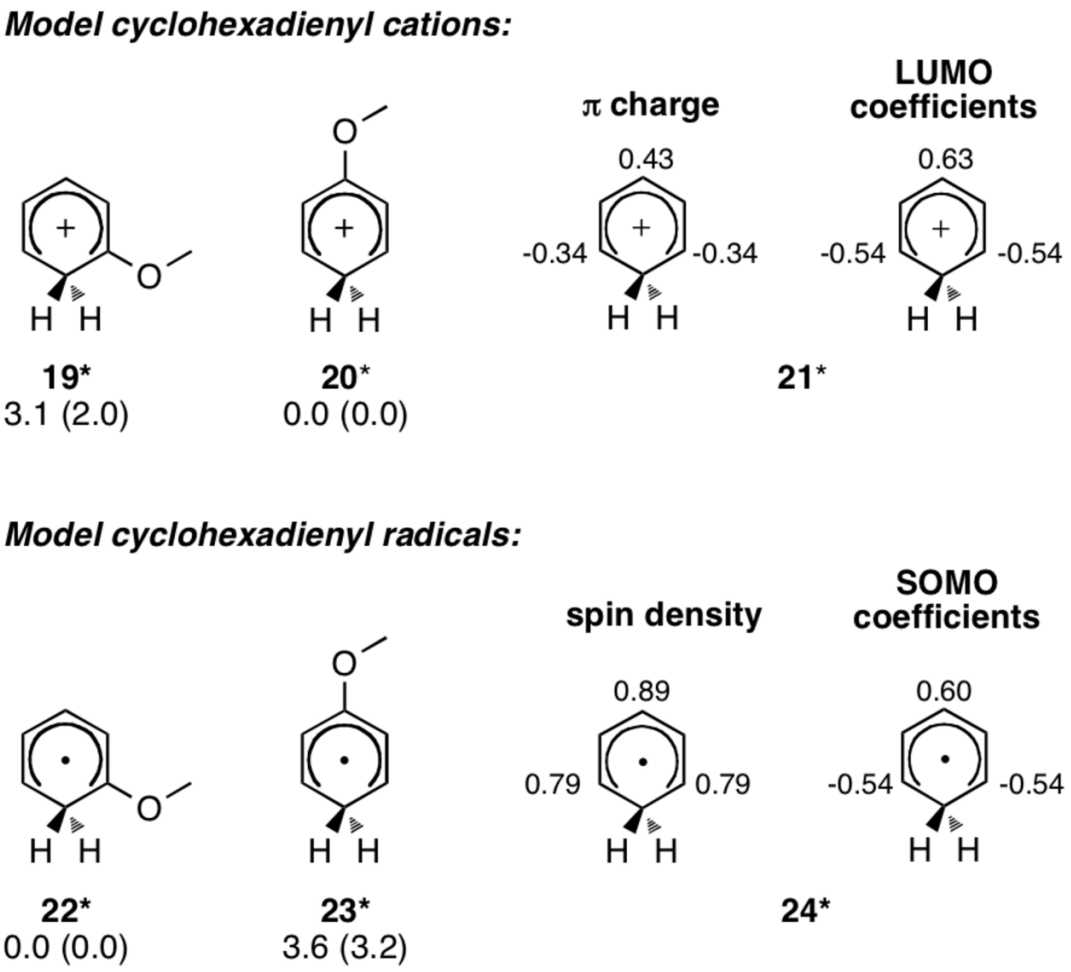

Figure 4.
Model *ortho*- and *para*-methoxy cyclohexadienyl cations and radicals. CBS-QB3 Δ*H*. B3LYP/6-31G(d) values in parentheses.

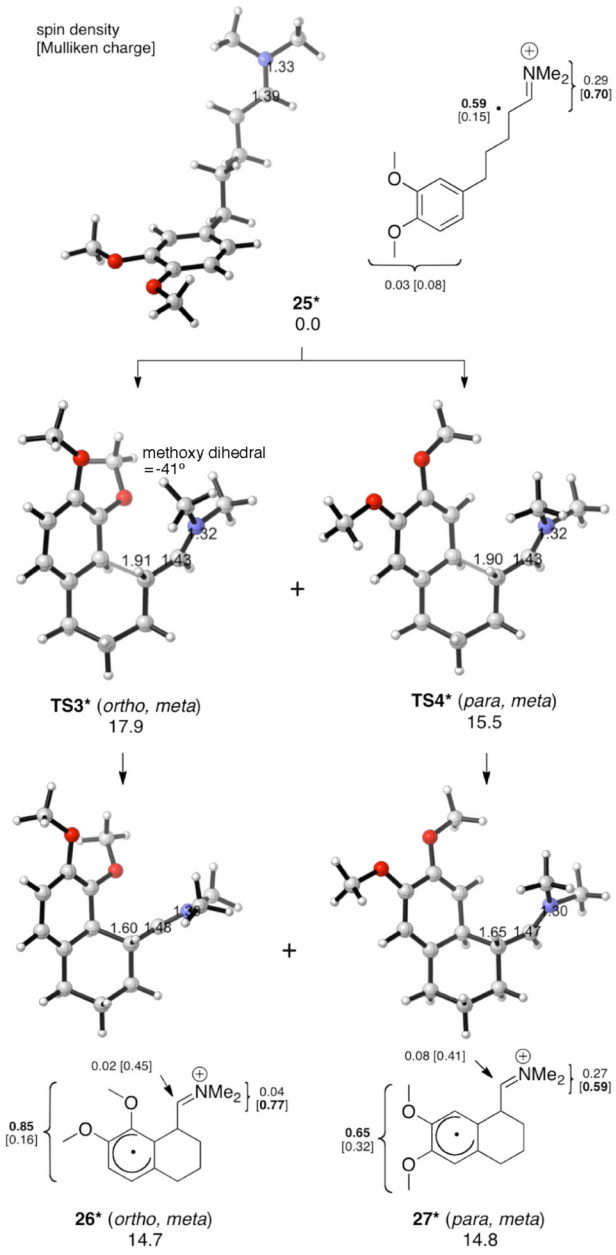

Figure 5.

Intramolecular α-arylation of **25*** (UB3LYP/6-31G(d) Δ*G* values for aqueous solution at 268 K; optimizations in CPCM water).

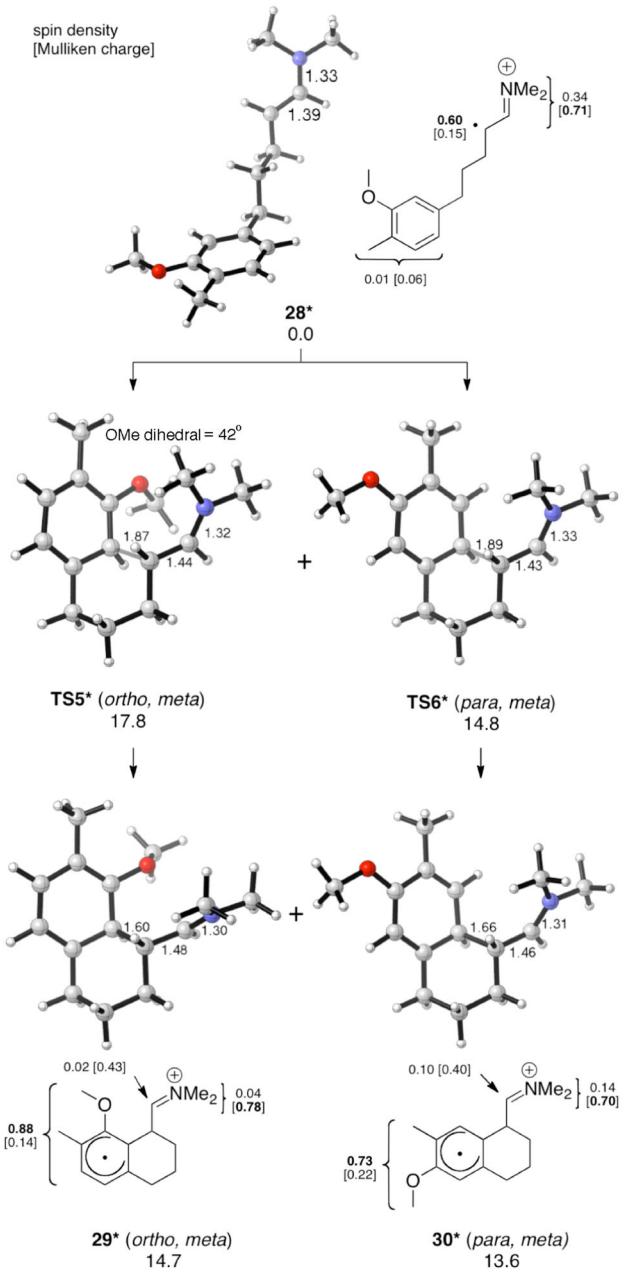

Figure 6.

Intramolecular α-arylation of **28*** (UB3LYP/6-31G(d) Δ*G* values for aqueous solution at 268 K; optimizations in CPCM water).

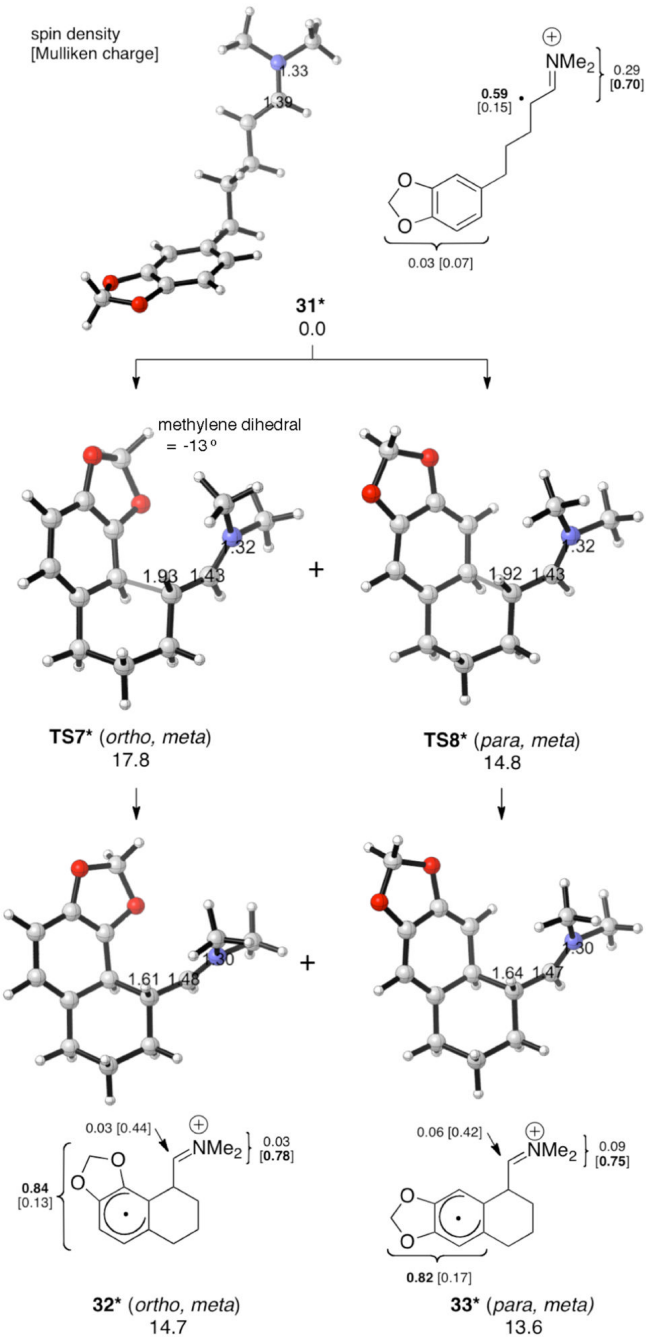

Figure 7.

Intramolecular α-arylation of **31*** (UB3LYP/6-31G(d) Δ*G* values for aqueous solution at 268 K; optimizations in CPCM water).

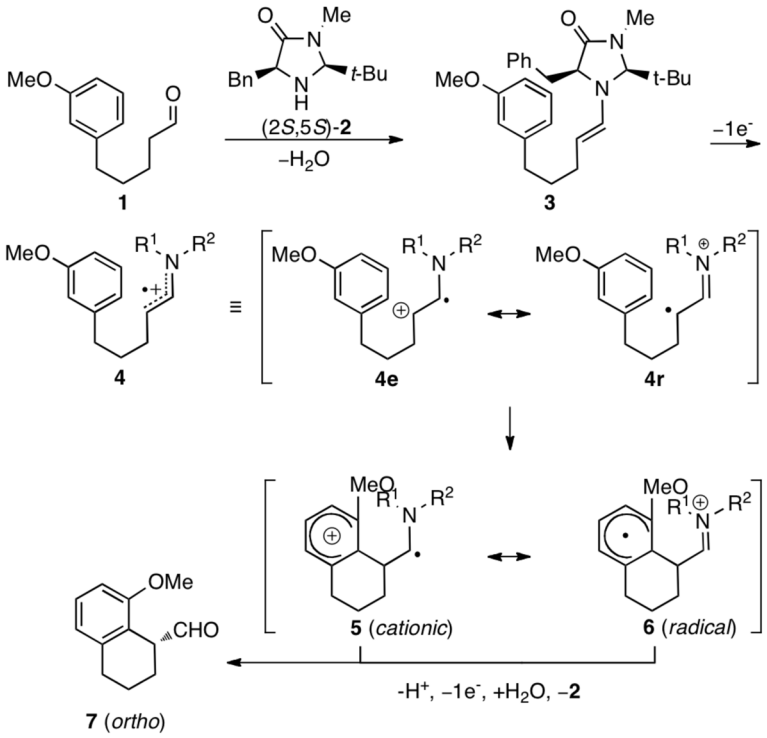

Scheme 1.

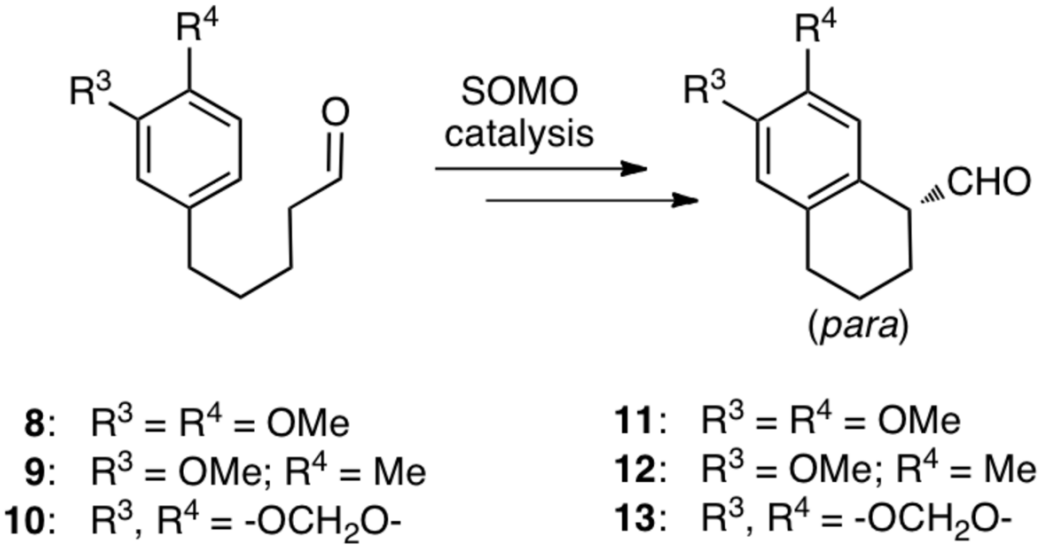

Scheme 2.

Table 1

Intramolecular α-arylation of aryl rings

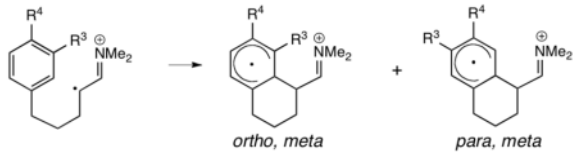

		UB3LYP/6-31G(d)[a]				M06-2X/6-31+G(d)[a,b]			
entry	**uncyclized radical cation**	**$\Delta G^{\ddagger}$*ortho*, (*meta*)**	**$\Delta G^{\ddagger}$*para*, (*meta*)**	**ΔG_{rxn}*ortho*, (*meta*)**	**ΔG_{rxn}*para*, (*meta*)**	**$\Delta G^{\ddagger}$*ortho*, (*meta*)**	**$\Delta G^{\ddagger}$*para*, (*meta*)**	**ΔG_{rxn}*ortho*, (*meta*)**	**ΔG_{rxn}*para*, (*meta*)**
1	R^3 = OMe, R^4 = H, **16***	15.2 **TS1***	15.7 **TS2***	12.2 **17***	15.1 **18***	12.1 **TS1***	13.6 **TS2***	6.1 **17***	10.5 **18***
2	R^3 = R^4 = OMe, **25***	17.9 **TS3***	15.5 **TS4***	14.7 **26***	14.8 **27***	14.7 **TS3***	12.4 **TS4***	9.0 **26***	8.9 **27***
3	R^3 = OMe, R^4 = Me, **28***	18.8 **TS5***	15.4 **TS6***	15.8 **29***	14.9 **30***	14.6 **TS5***	13.3 **TS6***	9.9 **29***	10.2 **30***
4	R^3, R^4 = –OCH_2O–, **31***	17.8 **TS7***	14.8 **TS8***	14.8 **32***	13.6 **33***	14.7 **TS7***	12.4 **TS8***	9.2 **32***	8.2 **33***
5	R^3 = R^4 = H, **34***	18.3, TS9*		16.0, 35*		16.0, TS9*		10.7, 36*	

[a] UB3LYP/6-31G(d) thermal corrections at 268 K have been applied.

[b] Reported values represent single point calculations of the UB3LYP/6-31G(d) optimized geometries.

Table 2

Comparison of dihedral angles (a-b-c-d) in *ortho, meta* TSs versus *ortho, meta* cyclized radical cations.

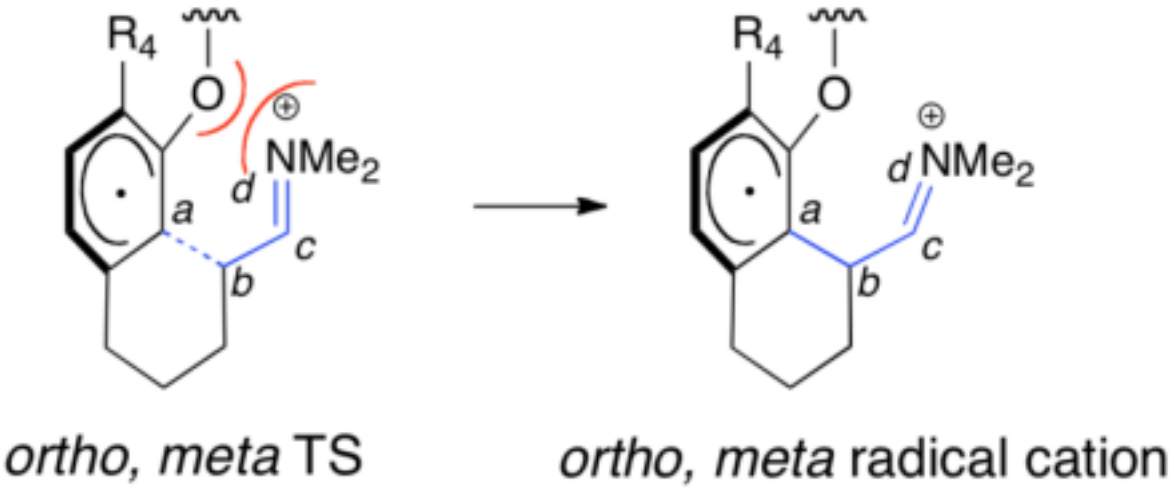

entry	R^3, R^4	TS dihedral angle (°)	Cyclized radical cation dihedral angle (°)
1	$R^3 = R^4 = OMe$	95, **TS3***	128, **26***
2	$R^3 = OMe$, $R^4 = Me$	95, **TS5***	119, **29** *
3	R^3, $R^4 = –OCH_2O–$	98, **TS7***	131, **32***